A Possible Mechanism for Electrocardiographically Silent Changes in Cardiac Repolarization

Robert S. MacLeod, Ph.D. Robert L. Lux, Ph.D. Bruno Taccardi M.D., Ph.D.*

Short titles: Detection of Repolarization Changes

Key words: electrocardiography, repolarization body surface potential mapping, ischemia

Address for correspondence: Dr. Robert S. Macleod, Nora Eccles Harrison CVRTI, Building 500, University of Utah, Salt Lake City, Utah.
Telephone: (801)581-8183, FAX: (801)581-3128,
Email: macleod@cvrti.utah.edu.

Support: Richard A. and Nora Eccles Harrison Treadwell Fund for Cardiovascular Research and awards from the Nora Eccles Treadwell Foundation. National Institutes of Health SCOR in Sudden Cardiac Death, HL 52338-01.

*Nora Eccles Harrison Cardiovascular Research and Training Institute, University of Utah, Salt Lake City, Utah

Abstract

Despite the widespread use of the ECG, changes in cardiac activity resulting from ischemia or altered recovery characteristics sometimes remain electrocardiographically "silent" or are first detectable using techniques that measures ventricular contractility such as ultrasound or blood pressure. Especially *local* changes in repolarization can go undetected when ECG electrodes do not lie close to the area of the heart affected. We have carried out experiments using an isolated, perfused canine heart suspended in a realistically shaped, instrumented, electrolytic torso tank with the goal of determining some mechanisms for these ambiguities. By recording simultaneously both epicardial and torso tank surface potentials, we obtained complete descriptions of the electrical response to interventions such as coronary occlusions and alterations in pacing site and frequency. One of our hypotheses was that some interventions produce highly variable electrocardiographic responses primarily because of differences in their location within the heart. To test this, we measured the effect of repeating the same intervention as we varied the heart's location and orientation in the tank. We have also used a numerical forward solution to investigate variation on torso tank potentials with heart location. The resulting changes in tank surface potentials illustrate how, for example, precordial ST-segment shifts following occlusion change from elevation, to depression, to become almost undetectable as the heart rotates in the tank. Our results suggest that some events are electrocardiographically silent because of the complex geometrical relationship of the heart, torso, and the site of the lesion as well as the spatial sampling and analysis techniques used in detection.

1 Introduction

Electrocardiographic potentials on the body surface result from a combination of components, many of which we understand only incompletely despite many years of research. Important clinical consequences are that the utility of the ECG is limited and that its limitations remain poorly characterized. In the specific case of detection of ischemia and infarction, emergency room diagnostic failure rates based on standard ECGs lie as high as 30% [1]. More fundamentally, there are numerous open hypotheses about the reasons why some ischemic events remain electrocardiographically silent, and what implications silent ischemia might have on clinical practice [2].

Percutaneous angioplasty (PTCA) has been a natural source of research data regarding the presence and electrocardiographic detection of ischemia [3]. Inflation of the angioplasty balloon takes a patient from a resting state, often in which no ischemia is detectable, to a state of acute ischemia under controlled conditions that permit repetition and extensive monitoring. However, here too there are many paradoxical findings of silent ischemia [4] or delays [5] in detection of ischemia, resulting in highly variable levels of detection of ischemia in different PTCA studies. One application of PTCA induced ischemia that underscores the difficulty of detecting ischemia in some patients is the use of an ECG "template" derived from recordings during PTCA as a means of improving the detection of subsequent ischemic episodes that would otherwise be overlooked by standard monitoring [6].

A recurring goal of research has been to understand fundamentally what factors determine the content of the body surface ECG. The articles of Holland, Brooks, and Arnsdorf form the basis of our understanding of the biophysics of electrocardiography [7, 8, 9]. Despite necessary modifications that take into account the electrically anisotropic nature of the heart tissue, the notions of the solid angle theory as described by these authors remain the underpinnings of our present knowledge. Many subsequent simulation studies have combined these ideas with physical laws of electrostatics and developed quantitative descriptions of the relationship between cardiac sources and body surface potentials, which is the *forward problem of electrocardiography* (for review, see [10]). Essential to each of the resulting formulations is a geometric description of the source, its distance from the sites of electrical measurement, and the shape of the volume conductor surrounding the heart. Because electric potential falls with distance (r) from the source as $1/r2$, even slight variations in lead/source configurations may have substantial effects on signals. The presence and shape of the outer boundary of the thorax brings about an increase in potential of some 2–3 fold over the (theoretical) case of a source in an infinite medium of the same conductivity [11].

The goal of this study was to isolate the effects of controlled variations in geometry on electrocardiographic potentials. To this end, we used simulation studies in the form of a numerical solution to the forward problem of electrocardiography, and experiments using a perfused isolated heart suspended in a torso shaped electrolytic tank. To focus the study on repolarization changes

during ischemia, we created acute occlusions of the left anterior descending artery and limited the analysis to deviations in ST segment potentials. In both the simulations and the experiments, we were able to rotate the heart during occlusion and observe the changes in tank surface potentials as a function *exclusively* of rotation angle.

2 Methods

2.1 Simulations

The goal of the simulations was to evaluate the effects of rotating the heart on the way the same distribution of epicardial potentials transferred to the tank surface. For this, we used a forward solution based on epicardial and torso tank surfaces and a numerical solution of Laplace's equation developed previously [12, 13]. Briefly, we begin with an integral equation relating potential anywhere in a piecewise homogeneous volume as a weighted sum of potentials on all the surfaces. For the simple case of epicardial and torso surfaces, the problem becomes homogeneous and the equation for potential anywhere in the volume can be expressed as

$$\phi(p) = \frac{1}{4\pi} \int_{S_H} \phi_H \, d\Omega - \int_{S_B} \phi_B \, d\Omega - \int_{S_H} \frac{\nabla \phi_H}{r} \cdot d\vec{A}, \tag{1}$$

where ϕ_H and ϕ_B are the epicardial and body (tank) surface potentials, $d\Omega$ is the incremental solid angle, $\nabla(1/r) \cdot d\vec{A}$, $\vec{A}$ is the surface normal vector, and r is the distance from the observation point p to the respective surfaces.

Solving this equation numerically (analytic solutions are impossible on all but the simplest geometries) for points on both surfaces leads to a matrix equation that encapsulates all the geometrical information into a set of weighting coefficients, which we can write as a matrix Z_{BH}. The relationship between epicardial and tank potentials is then

$$\Phi_B = Z_{BH} \Phi_H, \tag{2}$$

where Φ_B and Φ_H are the potentials from discrete points on the tank and heart surfaces expressed as a vector for each instant in time. The net result is that the potential at each point on the tank surface is a weighted sum of all the potentials from the epicardial surface; the weights–and hence Z_{BH}–depend only on the geometry and conductivity of the particular heart and volume conductor.

The geometric model required for this particular forward solution consisted of closed surfaces described as node locations in three-dimensional space and triangle connectivities. To form the tank surface geometry, we used a set of 658 surface points digitized directly from the torso tank during construction to which we then added planar, regularly spaced grids of points to close the cap and base. A subset of 192 nodes from the tank were also sites of recording electrodes, as described in the next section. To record the location of the heart surface, which changed for each

experiment, we first measured the location of the heart within the tank reference frame, and then removed the heart and digitized the locations of all 64 epicardial recording sites. A nonlinear fitting algorithm and a rigid body transformation using the *Procrustes* method [14] aligned the digitized heart surface to the proper location in the tank.

To create forward solutions for a range of heart orientations, we rotated the heart surface geometry in 10 degree increments about an axis aligned with the vertical tank axis running through the midpoint of the heart. Each orientation required a complete forward solution calculation and resulted in a unique forward coefficient matrix. Multiplying each matrix by the same set of epicardial potentials produced torso tank potentials that simulated those produced by rotating the actual heart.

2.2 Experiments

The experiments for this study served both to generate realistic geometry and epicardial potentials for the simulations, and to compare the results of the simulations with potentials recorded under similar conditions. The aim was to induce changes in repolarization through acute coronary occlusions and record simultaneously epicardial and tank surface potentials, while we then altered the location of the heart relative to the tank.

The preparation for the experiments consisted of an isolated dog heart, perfused by a second support dog and suspended in an instrumented electrolytic tank [15, 16]. The Utah torso tank is a fiberglass shell in the shape of an adolescent thorax filled with electrolyte of realistic conductivity (500 Ωcm). To record epicardial potentials, we used a nylon sock electrode array consisting of 64 silver wires knotted into the mesh and then slipped over the ventricles of the isolated heart. 192 Ag/AgCl pellets embedded in the inside of the shell detected tank surface potentials. Sampling rates were 1000 samples/s and a Wilson central terminal served as reference for the unipolar electrograms and ECGs.

To produce ischemic changes in repolarization, we isolated a 1-cm segment of the left anterior descending artery of the isolated heart, looped a suture silk around the artery and ran the ends through a 10–15 cm piece of tubing. This permitted repeated acute occlusions actuated from above the tank with the heart suspended in the electrolyte.

The experimental protocol in each experiment consisted of a sequence of occlusion "cycles", each of which included 3-4 minutes of complete occlusion followed by at least 10 minutes of recovery. We sampled all 256 channels simultaneously for 4-second bursts every 30 seconds through the first 6-8 minutes following onset of occlusion in each occlusion cycle. To measure the effect of changing heart position, we repeated occlusion cycles with the heart rotated in 90-degree increments. In a variation of this protocol, we and also carried out longer occlusions (up to 5 minutes) in which we recorded a 4-second epoch, then rotated the heart, recorded again, and so on. Such a series of rotations within a single occlusion cycle took 4-6 minutes to execute.

2.3 Data analysis

Standard preprocessing of the electrograms and tank ECGs consisted of gain adjusting each input signal, adjusting baselines, and selecting a representative beat for each recording burst, either through windowing or time aligned signal averaging. From an RMS curve for all the signals on each surface, we manually set fiducial markers for the onset and offset of the QRS and the end of the T wave.

For both simulations and experiments in this study, the aim was to examine specifically the changes in repolarization due to ischemia and heart rotation. This, combined with the need to analyze and present the large amount of data generated, motivated the use of the ST-segment integral as a data compression tactic. We defined the ST integral as the sum of the signal values times the sampling interval from each lead between the end of the (globally set for each surface) QRS and a time $3/8^{\text{th}}$ of the way from the end of the QRS to the end of the T wave. To compare simulations with experiments, the inputs to the forward solutions were epicardial ST integral values, thus producing simulated torso tank ST integrals.

First examination of the data was by isointegral maps either interactively on a three-dimensional model of the tank or epicardial surface [17], or by projected isocontour maps. In order to quantify the changes in repolarization, we computed histograms of the ST-integral values for each condition or simulation and compared their shapes and statistics. Reflecting clinical practice, we extracted the extrema of the ST-integral values both over the entire surface of the tank, and also over the subset of nodes corresponding to the standard ECG leads, and displayed these as functions of rotation angle and time.

3 Results

Figure 1 shows excerpted maps from a sequence of simulations for a complete rotation of the heart geometry within the tank model. Clearly seen is the migration of the area of positive ST-segment integral (region colored red) around the torso surface as the heart rotates. Of more importance with regard to detecting ischemia on the basis of ST segment deviations is the finding that the shape and amplitude of the positive region (and its reciprocal counterpart (in blue) on the opposite side of the torso) also changes with rotation. While large and sharply focused when projected to the anterior and left side at 0 and 90° of rotation, the positive area is smaller in amplitude and more diffuse when it appears on the back at 180 and 270°. An example of the experimental counterpart of these results is shown in Figure 2 for rotation of the heart during a single occlusion cycle. Epicardial potentials remained very consistent throughout the continuous occlusion while we rotated the heart in 90° increments. Measured torso tank potentials, similar to the simulation results, showed both a migration of the region of positive integral values as well as even more striking changes in amplitude and map pattern.

Please place Figures 1 and 2 here

Figure 3 contains another comparison between simulated and measured results in which we display the maximum and minimum values of the ST-segment integrals as functions of rotation. The simulation results in the left-hand panel indicate an overall fluctuation of some 15% in maximum ST-integral value with only a slight variation in the minimum; the peak ST-integral maximum amplitude appears between 20 and 40°, an orientation in which the epicardial ST-segment elevation is directed toward the anterior and left sides of the torso. The right-hand panel shows the corresponding measured values from the experiments for 0, 90, 180, 270, and 360 degrees of rotation. Here, the variation with rotation is much greater than in the simulations, with the maximum ST-integral elevation changing by a factor of 2 and showing a peak at 180 °of rotation.

Please place Figure 3 here

Variations in ST-segment integral value with rotation at specific sites corresponding to the standard ECG leads are shown in Figures 4 for simulated potentials and 5 for measured tank potentials. The simulated ST deviations in Figures 4 vary smoothly with rotation over a 2-3 fold range in amplitude in some leads (*eg.,* all precordial leads). The corresponding measured values in Figures 5 vary even more sharply with rotation; depending on orientation, ST-segment integral values can swing from almost zero to 150 μVs. At 270° of rotation, none of the precordial leads show more than 15 μVs of ST integral elevation or depression, one tenth of the value at 90°.

Please place Figures 4 and 5 here

To place the variations brought about *purely* by rotation of the heart in a relevant context, Figures 6 and 7 contain the same presentation as in the previous figures, but for the case of an acute occlusion of the left anterior descending artery. Here, the variation is not with rotation but with time over the course of the occlusion cycle. The vertical scales in Figure 3 match that in Figure 6, permitting direct comparison of the size of the fluctuations in ST-integral values. From this, it is clear that *rotation alone* during an stable occlusion leads to much larger fluctuations in ST-segment integral amplitude than the acute occlusion itself.

Please place Figures 6 and 7 here

4 Discussion

The aim of this study was to evaluate the hypothesis that variations in torso potentials brought about purely by the geometric arrangement of the heart and the torso surface might be large enough

to obscure the electrocardiographic signs of ischemia. Large variations in heart location do arise suddenly in nature, of course, but across patients, considerable differences in geometry do exist. Hence, one can imagine a situation of two patients with physiologically identical—or at least very similar—ischemic episodes appearing quite differently on the body surface. The result might be a different diagnosis, or in the extreme even a missed diagnosis. From a slightly different perspective, one can also imagine the effect not of the heart rotating in the torso, but of the ischemia arising in different regions of the heart. If the same degree of ischemia were present, the location and orientation of that ischemia could determine the manner and degree to which it is visible on the torso surface electrocardiogram. This too could lead to misdiagnosis.

In these experiments, we have used a moving heart with a fixed zone of ischemia as a surrogate for ischemia that arises in different parts of the stationary heart. Certainly the two situations are not complete analogs, however, keeping the physiology in a quasi-fixed state—or at least fixing the reflection of the physiology, the epicardial potentials—and varying only geometry, achieves a clean separation of physiological effects from purely spatial relationships. Hence, this study does not directly prove that the reason one case of ischemia might be clearly reflected from a standard ECG while another, similar case goes undetected because it arises in a less favorable location. It does, however, suggest that variations that arise in ECGs due purely to altered spatial relationships between the cardiac source and the body surface can be as large as, sometimes larger than, the variations due to acute ischemia in an experimental preparation.

Many studies have shown the superiority of body surface potential mapping over standard ECG in detecting electrophysiological events (*eg.,* [18, 19, 20]). In concordance with past results, the variations due to rotation seen in these studies are better characterized using an mapping technique than by examining the equivalent of a standard lead subset. It appears, however, that while a surface mapping approach permits more accurate observation of the changes brought about by geometric variation, it does not offer a simple means to adjust or compensate for these variations; the cause of the resulting diagnostic error is fundamental and not a product of limited measurements. The most direct means of compensating for the effects of geometry is to include it explicitly in the analysis technique. Inverse solutions, which seek to estimate cardiac source parameters from body surface potentials, explicitly include geometrical information, typically in the form of the associated forward solution (for reviews, see, for example, [12, 21, 22, 23]). While the accuracy and hence utility of a general purpose inverse solution has yet to reach acceptable levels, for cases in which geometrical effects obscure all traces of underlying pathophysiology, even a modest inverse solution could prove useful.

The use of simulations in this study had several goals and some limitations. Simulations allow for testing of a huge range of situations and conditions, both the number and difficulty of which often exceed experimental capabilities. In some cases, such as in human electrocardiographic studies, simulations can examine relationships completely unattainable to the experimentalist. In this

specific case, simulations allowed us to freely vary heart orientation and we have only just begun to tap the resulting possibilities. However, a simulation is only as good as its accuracy and the forward solution described here did not always reproduce measured results accurately. Instead, it served to suggest possible findings, most of which were not only reinforced, but actually enhanced, by the experiments. Fluctuations in potential amplitude and variation in map topography were in general larger in the experimental results than in the simulations.

We suspect at least three sources of error in the simulations, two inherent to the forward solution and a third specific to the rotation of the geometry. The forward solution requires a closed geometry and epicardial potentials that completely surround the heart. Our measurement sock, on the other hand, covers only the ventricles so that we must either interpolate over the surface enclosing the base of the heart, or leave this region sparely covered with model nodes. A second, related potential weakness lies in the limited spatial resolution of the 64-lead epicardial sock. Mean inter-electrode distance of such a sock lies in the range of 1-2.5 cm., well below the resolution required to capture even moderately detailed cardiac propagation behavior. Mitigating this limitation in the present study was the use of ST-integral values in the analysis; the spatial variation of this parameter is very gradual so that even a limited sampling resolution is likely to be adequate. The final limitation of the simulations was that the axis of rotation used to generate the geometries was not the same as that used in the experiments, but was derived from the midpoint of the heart surface points. Future experiments will include the measurements necessary to correct this omission.

Other simulations and experiments will be necessary to refine and quantify the effect of geometrical variation on ECGs, and especially the detection of phenomena such as ischemia from torso measurements of altered repolarization. Included must be the application of standard electrocardiographic techniques, modified for use in simplified conditions of the electrolytic torso tank. Only then can the hypothesis regarding the role of spatial location and orientation on electrocardiographically "silent" events be fully tested. These preliminary studies suggest that position can play a profound role in some electrocardiographic parameters and that the variations in these parameters are easily as large as those caused by the underlying pathophysiologic event. Both these results and our current understanding of the biophysics of electrocardiography support the suspicion that many apparently silent events are missed because either we are looking in the wrong place, or because factors such as distance and conductivity render the telltale signs too small to detect at the body surface. Both possibilities suggest that inverse solutions may play a useful role in separating the effects of geometry from true electrophysiologic events.

References

[1] H. P. Selker. Coronary care unit triage decision aids: How do we know when they work? *Am J Med*, 87:491–493, 1989.

[2] S. L. Bridges, J. S. Hollowell, S. W. Stagg, K. A. Kemle, M. L. Nusynowitz, D. C. Allensworth, D. B. Pryor, and J. R. Moorman. Is silent ischemia on the routine admission ECG an important finding? *J Electrocardiol*, 26(2):131–136, 1993.

[3] P. W. Serruys and G. T. Meester, editors. *Coronary Angioplasty: A Controlled Model for Ischemia*. Martinus Nijhoff Publishers, Dordrecht/Boston/Lancaster, 1986.

[4] D. Wohlgelernter, C. C. Jaffe, H. S. Cabin, L. A. Yeatmen, and M. Cleman. Silent ischemia during coronary occlusion produced by balloon inflation: Relation to regional myocardial dysfunction. *J Am Coll Cardiol*, 10:491–498, 1987.

[5] P. W. Serruys, W. Wijns, F. Piscione, F. ten Kate, P. de Feyter, M. van den Brand, and P. G. Hugenholtz. Early changes in wall motion and wall thickness during percutaneous transluminal coronary angioplasty in man. *Can J Cardiol*, Suppl.:221A–232A, July 1986.

[6] M. W. Krucoff, Y. R. Jackson, M. K. Kehoe, and K. M. Kent. Quantitative and qualitative ST segment monitoring during and after percutaneous transluminal coronary angioplasty. *Circulation*, 80(supp IV):IV–20–IV–26, 1990.

[7] R. P. Holland and H. Brooks. The QRS complex during myocardial ischemia: An experimental analysis in the porcine heart. *J Clin. Invest.*, 57:541–550, 1976.

[8] R. P. Holland and H. Brooks. TQ-ST segment mapping: Critical review and analysis of current concepts. *Am J Cardiol*, 4:110–129, 1977.

[9] R. P. Holland and M. F. Arnsdorf. Solid angle theory and the electrocardiogram: physiologic and quantitative interpretations. *Progress in Cardiovascular Diseases*, 19(6):431–457, 1977.

[10] R. M. Gulrajani, F. A. Roberge, and G. E. Mailloux. The forward problem of electrocardiography. In P. W. Macfarlane and T. D. Veitch Lawrie, editors, *Comprehensive Electrocardiology*, pages 197–236. Pergamon Press, Oxford, England, 1989.

[11] R. Plonsey and R. C. Barr. *Bioelectricity: A Quantitative Approach*. Plenum Publishing, New York, London, 1988.

[12] Y. Rudy and B. J. Messinger-Rapport. The inverse solution in electrocardiography: Solutions in terms of epicardial potentials. *CRC Crit Rev Biomed Eng*, 16:215–268, 1988.

[13] R. S. MacLeod, R. M. Miller, M. J. Gardner, and B. M. Horáček. Application of an electrocardiographic inverse solution to localize myocardial ischemia during percutaneous transluminal coronary angioplasty. *J Cardiovasc Electrophysiol*, 6:2–18, 1995.

[14] J. H. Challis. A procedured for determining rigid body transformation parameters. *J. Biomechanics*, 28(6):733–737, 1995.

[15] R. S. MacLeod, B. Taccardi, and R. L. Lux. Electrocardiographic mapping in a realistic torso tank preparation. In *IEEE Engineering in Medicine and Biology Society 17th Annual International Conference*, pages 245–246. IEEE Press, 1995.

[16] R. S. MacLeod, R. L. Lux, M. S. Fuller, and B. Taccardi. Evaluation of novel measurement methods for detecting heterogeneous repolarization. *J Electrocardiol*, 29 Suppl.:145–153, 1996.

[17] R. S. MacLeod and C. R. Johnson. Map3d: Interactive scientific visualization for bioengineering data. In *IEEE Engineering in Medicine and Biology Society 15th Annual International Conference*, pages 30–31. IEEE Press, 1993.

[18] D. M. Mirvis. Body surface distributions of replarization potentials after acute myocardial infarctions. II. Relationship between isopotential mapping and ST-segment potential summation methods. *Circulation*, 63(3):623–631, 1981.

[19] R. L. Kornreich, F. ad Lux and R. S. MacLeod. Map representation and diagnostic performance of the standard 12-lead ECG. *J Electrocardiol*, 28 Suppl.:121–123, 1995.

[20] L. S. Green, R. L. Lux, and C. W. Haws. Detection and localization of coronary artery disease with body surface mapping in patients with normal electrocardiograms. *Circulation*, 76:1290–1297, 1987.

[21] R. M. Gulrajani, F. A. Roberge, and P. Savard. The inverse problem of electrocardiography. In P. W. Macfarlane and T. D. Veitch Lawrie, editors, *Comprehensive Electrocardiology*, pages 237–288. Pergamon Press, Oxford, England, 1989.

[22] L. S. Green, R. L. Lux, P. R. Ershler, R. A. Freedman, F. I. Marcus, and K. Gear. Resolution of pace mapping stimulus site separation using body surface potentials. *Circulation*, 90:462–468, 1994.

[23] R.S. MacLeod and D.H. Brooks. Recent progress in inverse problems in electrocardiology. *IEEE Eng. in Med. & Biol. Soc. Magazine*, (in press), 1997.

Figures

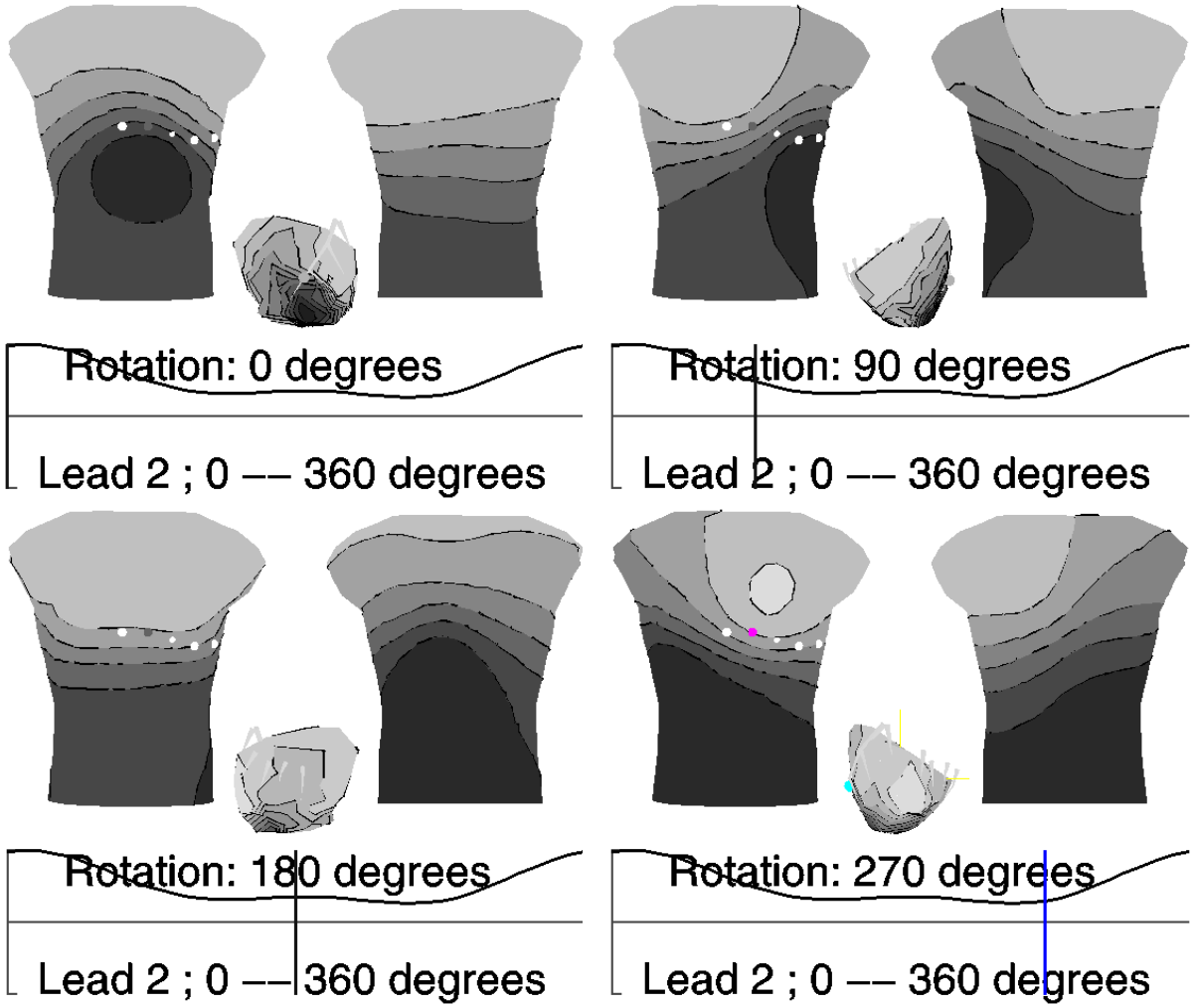

Figure 1: Simulated forward solutions. Each of the four panels contains images of computed tank surface iso-integral maps, in both anterior and posterior views. Between views of the torso is a display of the epicardial surface oriented as it was in the associated simulation. Colors on the surfaces indicate the value of ST-segment integrals with the scale in the upper left-hand panel showing the mapping for the torso surfaces. The label above the scalar tracing at the bottom of each panel indicates the heart surface rotation, as does the location of the vertical line in the tracing. White circles marks the approximate locations of standard precordial leads.

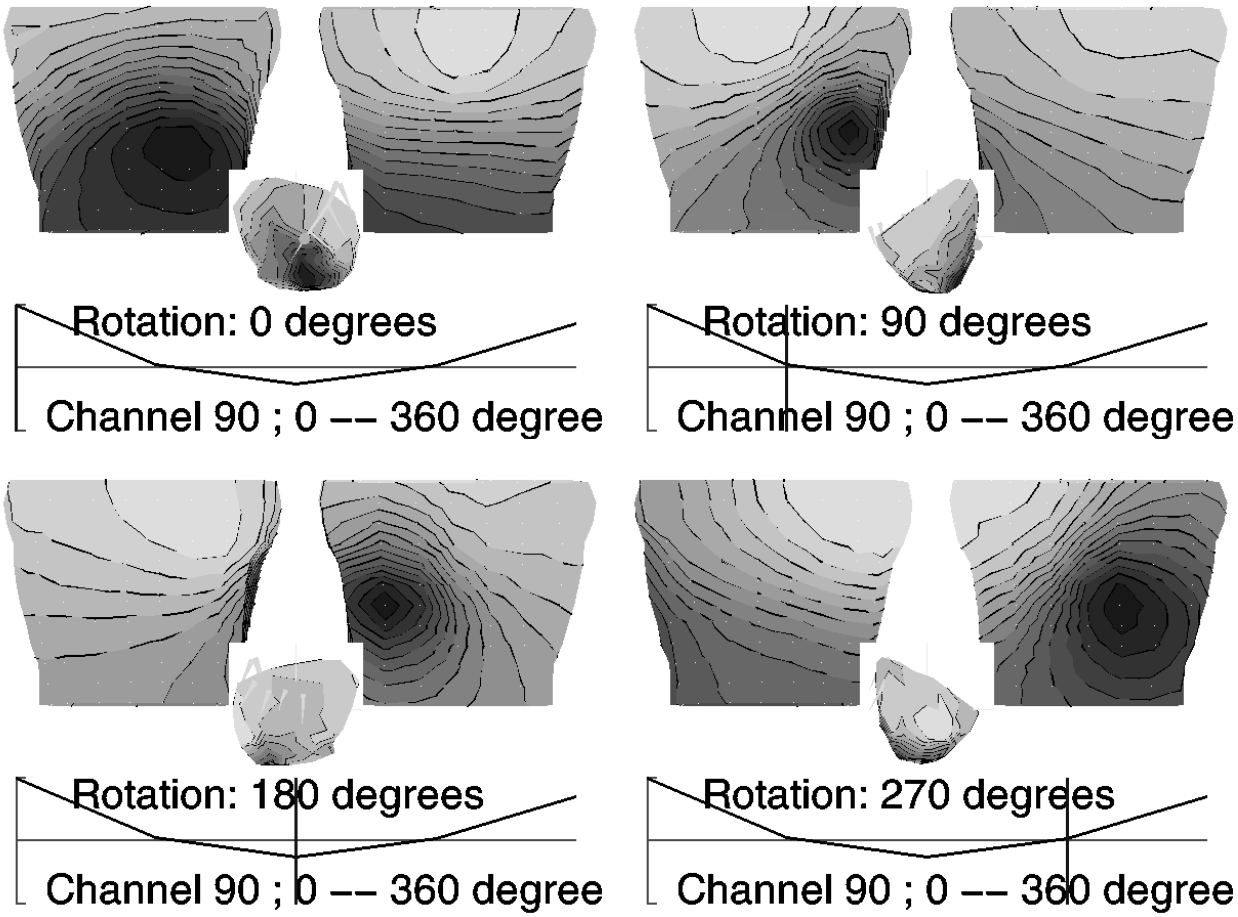

Figure 2: Measured tank potentials during rotation. Each panel contains images of measured tank surface iso-integral maps, in both anterior and posterior views, as well as the simultaneously measured epicardial potentials (arranged as in the previous figure). In this case, both the epicardial and tank potentials changed at each orientation. Isointegral values are for the ST segment, displayed with a similar coding scheme as in the previous figure.

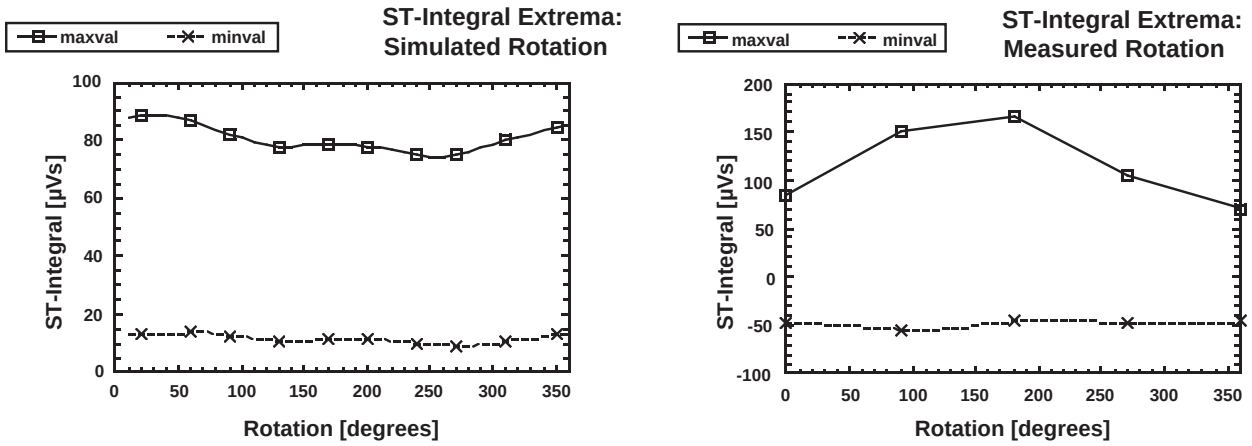

Figure 3: ST-integral extrema as functions of rotation angle. The left-hand panel contains the ST-integral maximum and minimum for simulated torso tank potentials while the right-hand panel contains the measured counterparts.

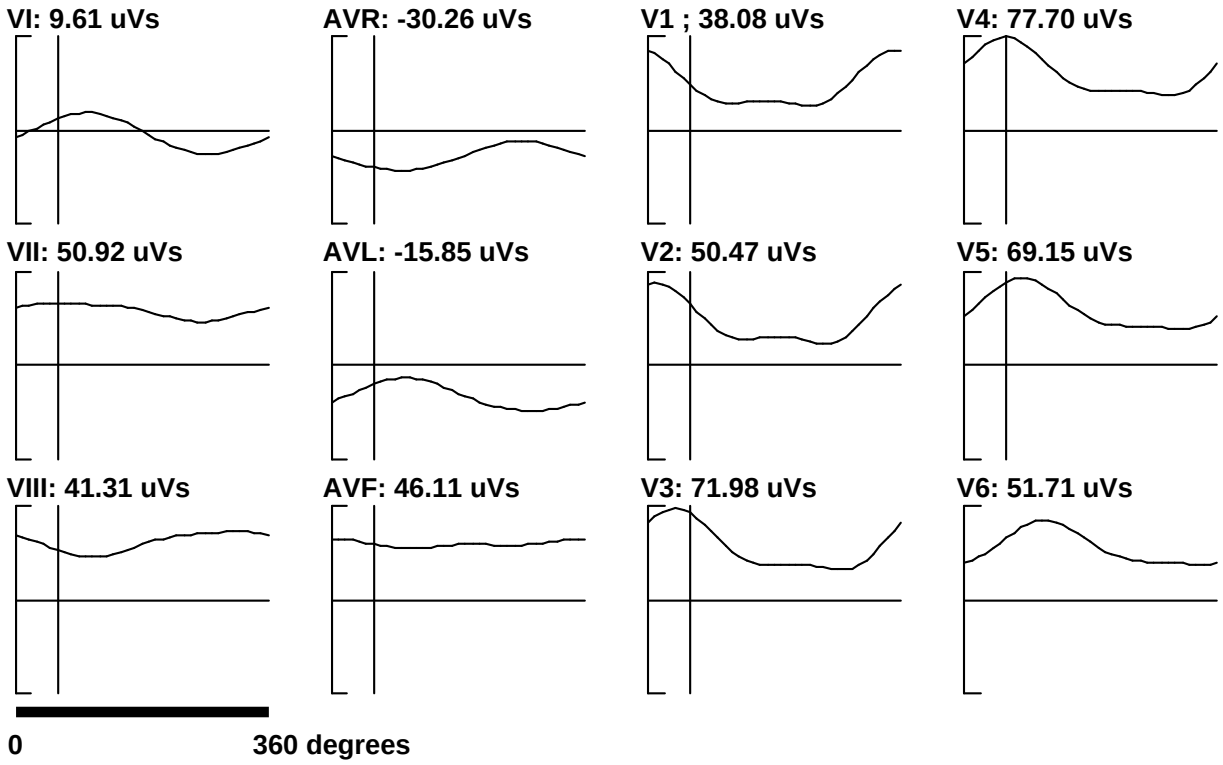

Figure 4: ST-integral values for standard ECG leads as a function of rotation for **simulated** ST integrals over the full rotation of the heart. Vertical scaling is identical for each lead and the labeled values indicate the ST-integral values at the angle marked by the vertical line in each lead. The horizontal axis sweeps through 360 degrees, as indicated in the lower left corner of the display.

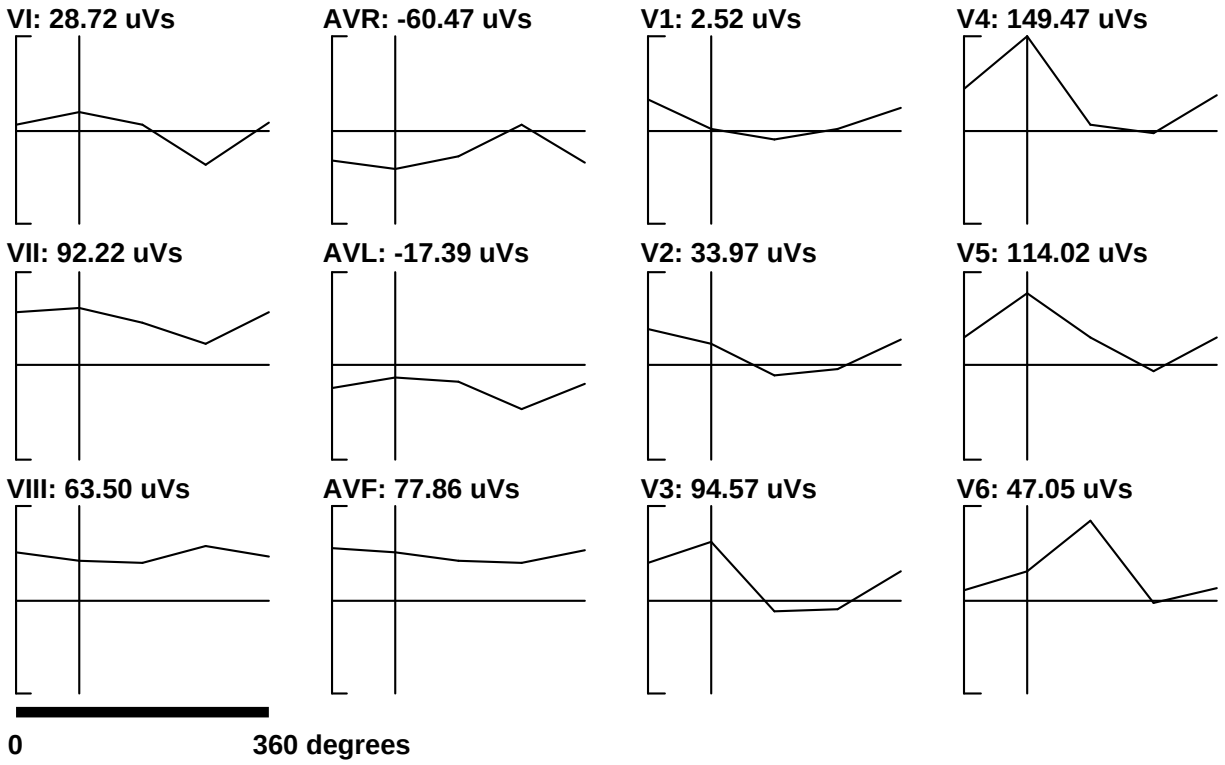

Figure 5: ST-integral values for standard ECG leads as a function of rotation for **measured** ST integrals over the full rotation of the heart. Layout is identical to that in the previous figure.

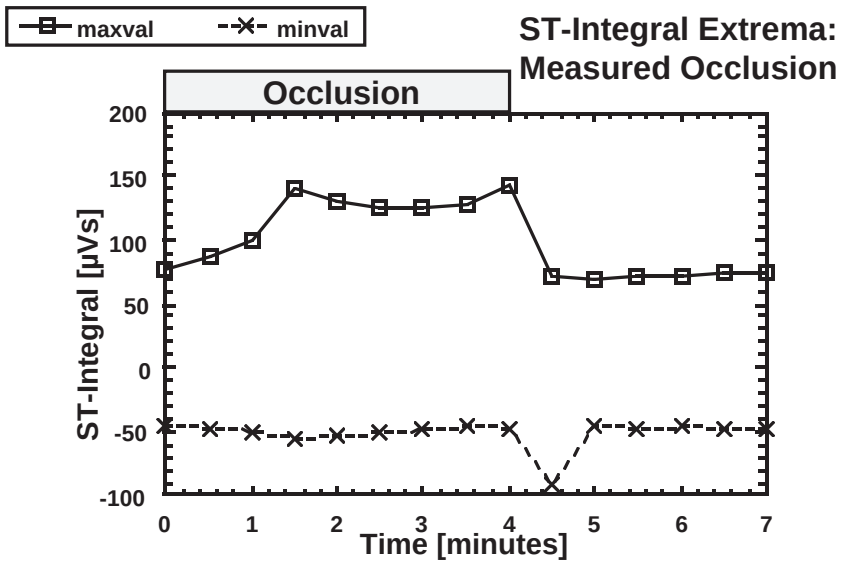

Figure 6: ST-integral extrema as functions of time for an occlusion cycle. ST-integral extrema are shown for each of a series of recorded beats throughout a complete occlusion/release cycle. Scaling is identical to that in the corresponding figure for rotation and the duration of occlusion is marked by a shaded rectangular above the graph.

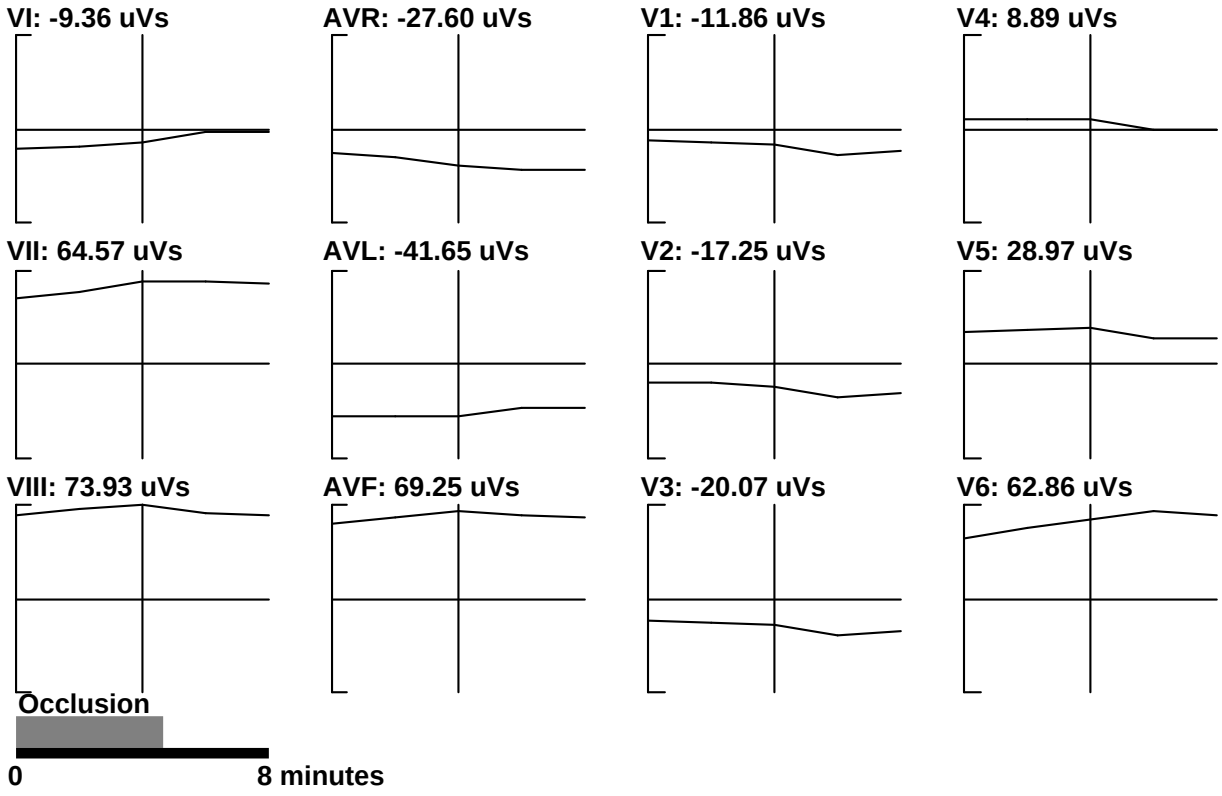

Figure 7: ST-integral values for standard ECG leads as a function of time for the same occlusion cycle as in previous figure. The values for the ST integral are shown for standard leads as functions if time. Duration of the occlusion is marked in the time bar at the bottom left corner of the figure